Morphological Considerations on the Mechanical Properties of Blown High-Density Polyethylene Films

YONG-MAN KIM,[1] CHUL-HWAN KIM,[1] JUNG-KI PARK,[1,*] CHEOL-WOO LEE,[2] and TAE-IK MIN[2]

[1]Department of Chemical Engineering, Korea Advanced Institute of Science and Technology, 373-1, Kusung-dong, Yusung-gu, Daejon, 305-701, and [2]Central Research Center, Hanwha Chemical Corporation, 6, Shinsung-dong, Yusung-gu, Daejon, 305-345, Korea

SYNOPSIS

Blown films having a broad range of morphologies were prepared from high-density polyethylenes (HDPE) with unimodal and bimodal molecular weight distribution under several processing conditions, and the effect of their morphological features on the dart drop impact resistance, Elmendorf tear strength, and tensile properties of the films has been studied. The organization of lamellar stacks seems to play a critical role on the mechanical properties of the blown HDPE films. The dart drop impact resistance of the blown HDPE films is highly dependent on the presence of the network structure of lamellar stacks and the level of the intraconnectivity and interconnectivity of lamellar stacks. The coherent orientation of lamellar stacks leads to significant anisotropy of tear and tensile properties. © 1997 John Wiley & Sons, Inc.

INTRODUCTION

There has been considerable interest in the mechanical properties of blown high-density polyethylene (HDPE) films, because it is one of the most widely used polymeric products. The most important mechanical properties of blown HDPE films are dart drop impact resistance, Elmendorf tear strength, and tensile properties.

The mechanical properties of blown HDPE films are highly associated with their morphological features, which are dependent on the overall processing conditions as well as the molecular characteristics of HDPE resins. Some correlations were found between the anisotropy of the tear and tensile properties of blown HDPE films and the state of orientation of the crystalline molecular chain axes[1–5] and lamellar stacks[6–9] at the film plane. Few studies have investigated the dart drop impact resistance of blown HDPE films. Recently, a superior dart drop impact resistance of the bimodal molecular weight distribution (MWD) HDPE film compared with the unimodal MWD HDPE film was reported.[10] Nevertheless, the underlying mechanics for this phenomenon has not been clear.

In this study, the effect of morphology on the above mechanical properties of the blown HDPE films prepared from the bimodal and unimodal MWD HDPE resins was comprehensively investigated. The details on the level of crystallinity, stacked lamellar crystalline morphology, intercrystalline connectivity, and preferred orientation of these films were already reported in the preceding article.[11] It is the purpose of this study to present some morphological observations which may shed light on our understanding of the mechanical properties of blown HDPE films.

EXPERIMENTAL

Materials

Eight tubular blown films were prepared from four commercial HDPEs, labeled BH, UH, BM, and UM, with 40-mm Yoo Jin Engineering HDPE film equipment. Some important properties of the resins and film-blowing conditions are summarized in Table I. Density and melt indexes were

* To whom correspondence should be addressed.

Journal of Applied Polymer Science, Vol. 63, 289–299 (1997)
 CCC 0021-8995/97/030289-11

Table I Preparation of the Blown HDPE Films

	Bimodal MWD[a]				Unimodal MWD			
	BH			BM	UH			UM
Resin								
Melt index, (g/10 min)								
I[b] 2.16	0.05			0.32	0.07			0.42
I[c] 21.6	8.5			27.7	10.5			32.6
Density[d] (g/cm^3)	0.9535			0.9551	0.9532			0.9535
Film	BH-1	BH-2	BH-3	BM-3	UH-1	UH-2	UH-3	UM-3
Thickness (μm)	23	23	23	24	20	22	23	23
Blow-up ratio	5.0	2.5	2.5	2.5	5.0	2.5	2.5	2.5
Draw ratio	7.4	14.6	14.4	13.7	7.5	13.8	14.8	14.4
Frost-line height (cm)	53	53	26	25	53	54	25	25

[a] Molecular weight distribution.
[b] ASTM D 1238 (condition E).
[c] ASTM D 1238 (condition F).
[d] ASTM D 1505.

measured according to ASTM D 1505 and D 1238, respectively. The resins BH and BM have a bimodal MWD, while the resins UH and UM have a unimodal MWD. The films BH-1, BH-2, and BH-3 were made from the high-molecular-weight (HMW) resin BH under three sets of blowing parameters—draw ratio, blow-up ratio (BUR), and frost-line height (FLH). The processing condition of the film BH-1 is a commercially typical one. For the film BH-2, the stretching along the machine direction (MD) was increased while that along the transverse direction (TD) was decreased compared with the film BH-1. The blowing condition of the film BH-3 is very similar to that of the film BH-2 except for the lower FLH. The processing condition of the HMW UH resin films UH-1, UH-2, and UH-3 is almost the same as that of the HMW BH resin films BH-1, BH-2, and BH-3, respectively. The films BM-3 and UM-3 were respectively prepared from the medium molecular weight (MMW) resins BM and UM under processing conditions similar to that of the film BH-3. Detailed information on the molecular structure of the four resins and the conditions for film preparation was described in the previous study.[11]

Scanning Electron Microscopy

The crystalline morphology of the failed specimens obtained from dart drop impact resistance and Elmendorf tear strength measurements was investigated with Phillips SEM 535M. The specimens were etched with a 0.7 wt % solution of KM_nO_4 in a 2 : 1 (v/v) mixture of concentrated sulfuric acid and 98% phosphoric acid for 1 h at room temperature. The etched specimens were washed with a 2 : 7 (v/v) mixture of concentrated sulfuric acid and water, then washed with water again, and finally freeze dried. They were mounted on scanning electron microscopy (SEM) stubs with double-stick tape and sputter coated with gold. Accelerating voltage, probe current, and tilt angle were 7 kV, 3×10^{-11} mA, and 30°, respectively.

Mechanical Testing

Dart drop impact resistance was measured according to ASTM D 1709 (method A). Elmendorf tear strength was determined by ASTM D 1922 (rectangular specimen). ASTM D 882 was used for measuring the stress-strain behavior, yield strength, tensile strength, and percent elongation at the break of the films (initial strain rate = 10 mm/mm · min).

RESULTS AND DISCUSSION

Dart Drop Impact Resistance

The dart drop impact strength data on all of the films are given in Table II. The films UH-2, UH-3, BM-3, and UM-3 showed a lower dart drop impact resistance than the minimum weight (30 g) of the dart. The dart drop impact resistance of the films depends significantly on the overall blowing conditions as well as the used resins. It can be found

Table II Mechanical Properties of the Films

Film		BH-1	BH-2	BH-3	UH-1	UH-2	UH-3	BM-3	UM-3
Dart drop impact strength (g)		214	43	55	52	< 30[a]	< 30[a]	< 30[a]	< 30[a]
Elmendorf tear strength (g)	MD	18.7	7.2	11.7	16.6	8.9	8.6	10.5	10.7
	TD	111	797	717	93.4	887	755	780	837
Yield strength (kg/cm^2)	MD	270	442	304	275	426	409	264	272
	TD	217	190	192	210	184	165	195	177
Break strength (kg/cm^2)	MD	543	661	590	483	502	512	499	457
	TD	463	412	424	416	365	316	281	250
Elongation (%)	MD	440	260	300	380	250	270	410	450
	TD	540	770	730	660	780	768	740	760

[a] Less than the minimum weight of the dart (30 g).

that dart drop impact strength increased with an increase in BUR (a more balanced MD/TD stretching) and with an increase in molecular weight. It is also noted that the HMW bimodal resin BH film has a higher dart drop impact resistance than does the HMW unimodal resin UH film prepared under very similar processing conditions.

Figure 1 illustrates that the impact failure of the film BH-1 having the highest dart impact resistance occurred homogeneously at the film plane while those of the other films took place locally along the MD. In order to understand on a structural level this difference in the dart drop impact resistance of the films, the detailed morphology of the failure regions was investigated by the use of SEM. The scanning electron micrographs of all of the films are presented in Figures 2–4. The MD and TD are the vertical and horizontal directions of the micrographs, respectively. These micrographs clearly show the deformation behavior of the films resulting from the impact of a free-falling dart.

Figure 2(a) reveals the initial (intact) morphol-

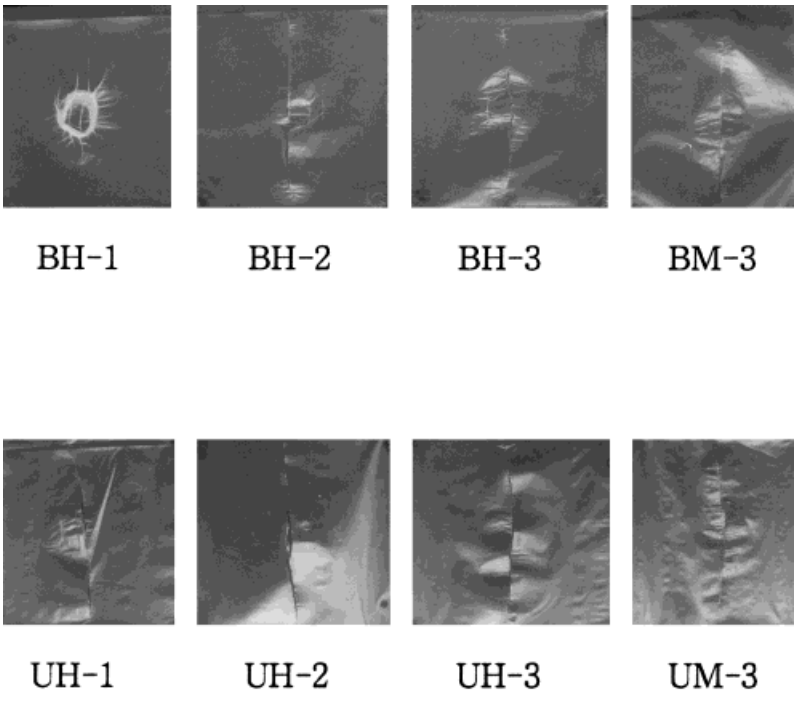

Figure 1 Photographs of the dart drop impact failure specimens of the films (MD↑, TD→).

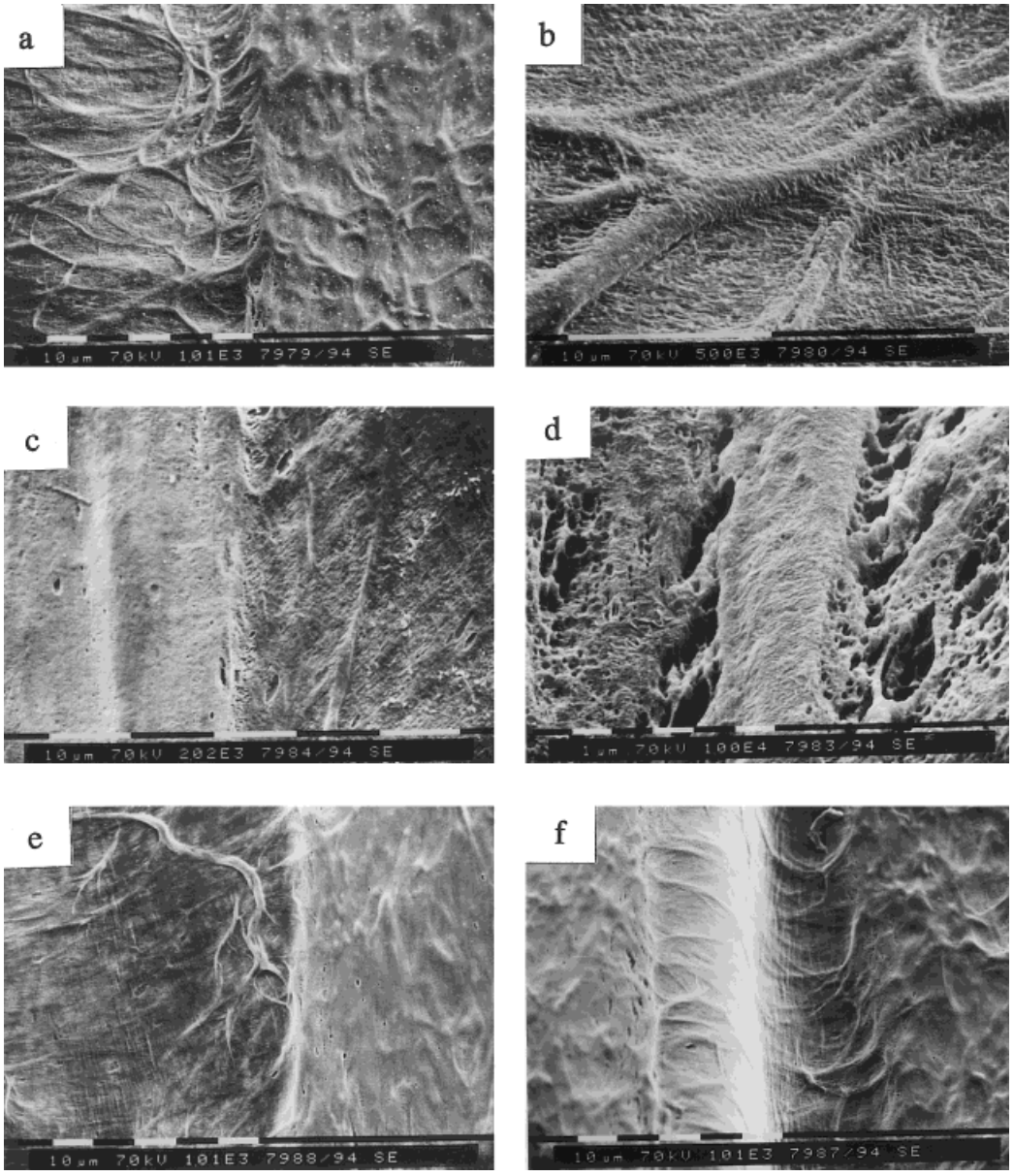

Figure 2 Scanning electron micrographs of the dart drop impact failure region of the resin BH films (MD↑, TD→): (a) BH-1, 1,000×; (b) enlarged micrograph of a deformed area from panel (a), 5,000×; (c) BH-2, 2,000×; (d) an area of the failure end of BH-2, 10,000×; (e) BH-3 (a rotation of a well-developed lamellar stack is clearly seen), 1,000×; (f) BH-3, 1,000×.

ogy of the film BH-1 and its deformation at a magnification of 1,000×. The film BH-1 has an obvious stacked lamellar morphology, as shown on the right side of the micrograph. The well-developed long lamellar stacks are curled and interconnected, forming a network just like a fishnet in the film. These lamellar stacks are 1–3 μm wide and 5–20 μm long between intersections or junctions with other stacks in the network. The surface normals of the network lamellar stacks are rather randomly distributed at the film plane. In addition to these network lamellar stacks, the lamellar stacks with narrower width are developed in the interstices of the network. The surface normals of these interstitial lamellar stacks are preferentially oriented to the MD. A failure boundary line parallel to the MD is shown at the center of the micrograph [Fig. 2(a)], and the detailed morphology of the deformed region is shown on the left

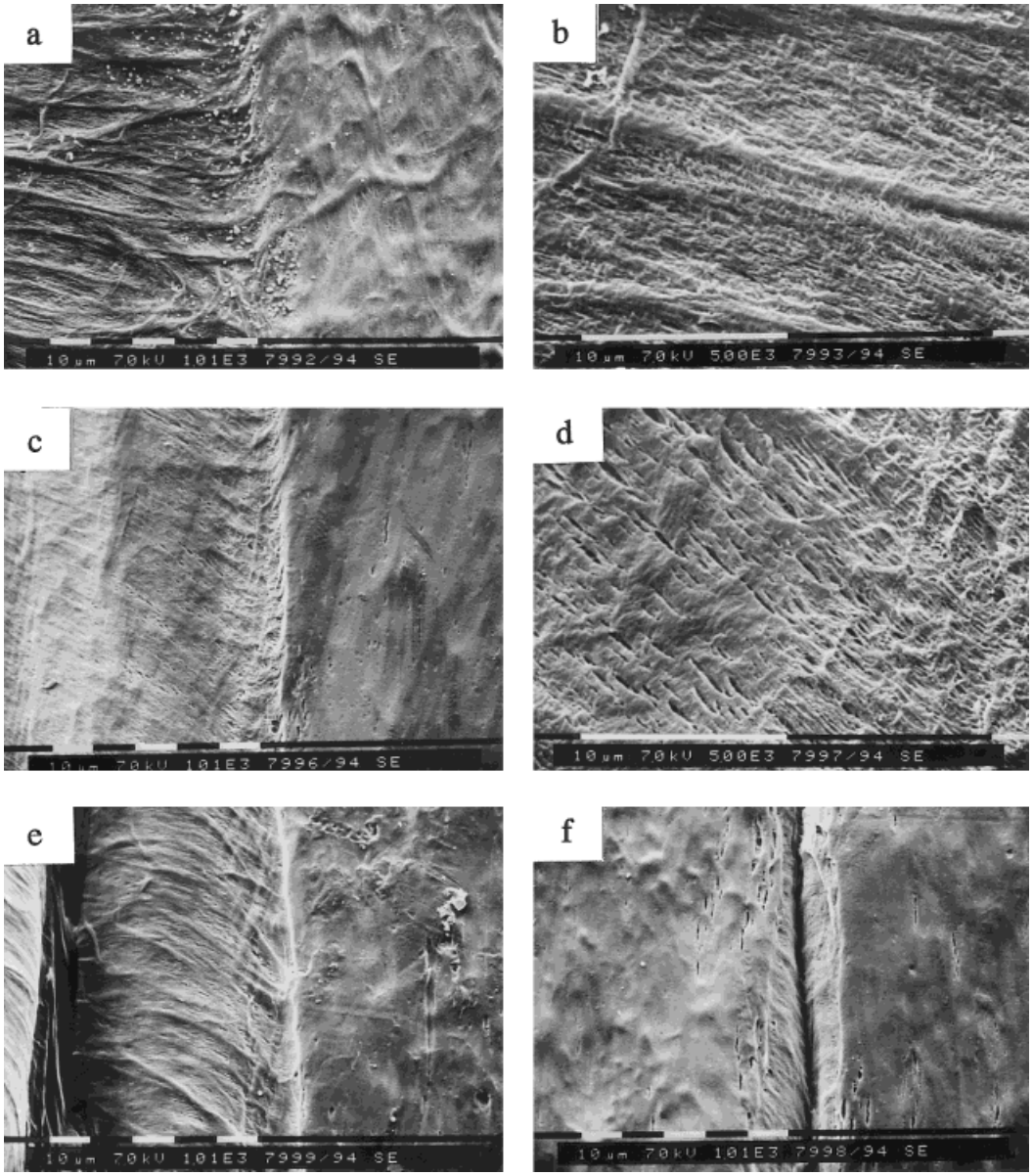

Figure 3 Scanning electron micrographs of the dart drop impact failure region of the resin UH films (MD↑, TD→): (a) UH-1, 1,000×; (b) enlarged micrograph of a deformed area from panel (a), 5,000×; (c) UH-2, 1,000×; (d) enlarged micrograph of a deformed area from panel (c), 5,000×; (e) UH-3, 1,000×; (f) UH-3 (the initial morphology is shown), 1,000×.

side of the micrograph. It is found that the well-developed network lamellar stacks are separated and then rotated perpendicular to the failure line. The axial deformation of them seems to be insignificant, as shown in Fig. 2(b), the higher magnification micrograph being taken by zooming up around a deformed area in the low-magnification micrograph [Fig. 2(a)]. The other interesting feature observed is the formation of fully deformed fibrous morphology in the interstices of the network lamellar stacks. These results imply that the region between the lamellar stacks is weak and that the interstitial lamellar stack is less stable than the network lamellar stacks. The above impact failure behavior of the film BH-1 is homogeneous at the film plane (Fig. 1), although the MD failure is only presented as the representative in this article. The network structure seems to be responsible for the homogeneous failure of the film BH-1, i.e.,the higher dart drop impact strength of the film BH-1.

Figure 2(c) exhibits the initial morphology (left side) of the film BH-2 and its deformation. Figure

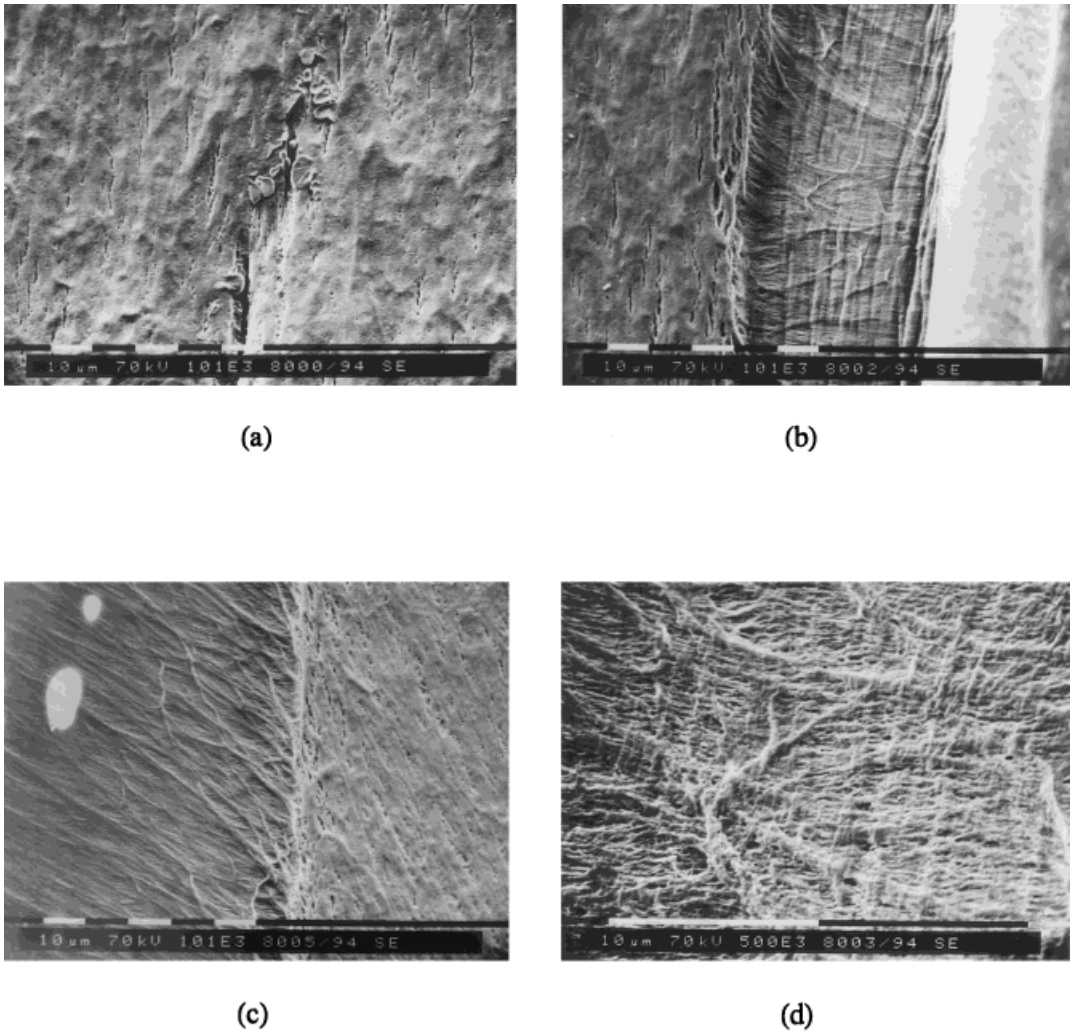

Figure 4 Scanning electron micrographs of the dart drop impact failure regions of the resin BM and UM films (MD↑, TD→): (a) an area of the failure end of BM-3, 1,000×; (b) BM-3, 1,000×; (c) UM-3, 1,000×; (d) enlarged micrograph of a deformed area from panel (c), 5,000×.

2(d) reveals an area of failure end of the film BH-2. The film BH-2 shows lamellar stacks to be highly ordered, with their normals along the MD. It is apparent from the two micrographs that in the initial stage of dart drop impact failure, the lamellar stacks are separated. This is followed by a reorientation of the lamellar stacks to the strain direction, resulting in the formation of microfibrils. The axial deformation of the well-developed lamellar stacks is not significant, as shown in Figure 2(c) and (d). The higher coherent orientation of the lamellar stacks to the MD seems to result in a local failure along the MD.

Figure 2(e) and (f) are SEM images taken from two parts in the failure region of the film BH-3. The deformed regions are shown on the left side of the micrograph presented in Figure 2(e) and at the center region of the micrograph shown in Figure 2(f). The film BH-3 also shows a local failure along the MD. This appears to be attributed to the poor development of network structure and the higher preferential orientation of lamellar stacks.

The scanning electron micrographs of the HMW unimodal resin films UH-1, UH-2, and UH-3 are presented in Figure 3. The initial morphology of the films UH-1, UH-2, and UH-3 is shown on the right side of the micrographs presented in Figure 3(a), (c), and (e), respectively. Figure 3(b) and (d) are enlarged micrographs of the deformed regions from Figure 3(a) and (c), respectively. The initial morphology of the film UH-3 is more clearly shown on the left side of the micrograph presented in Figure 3(f) than on the right side of the micrograph shown in Figure 3(e). The dependency of the morphology

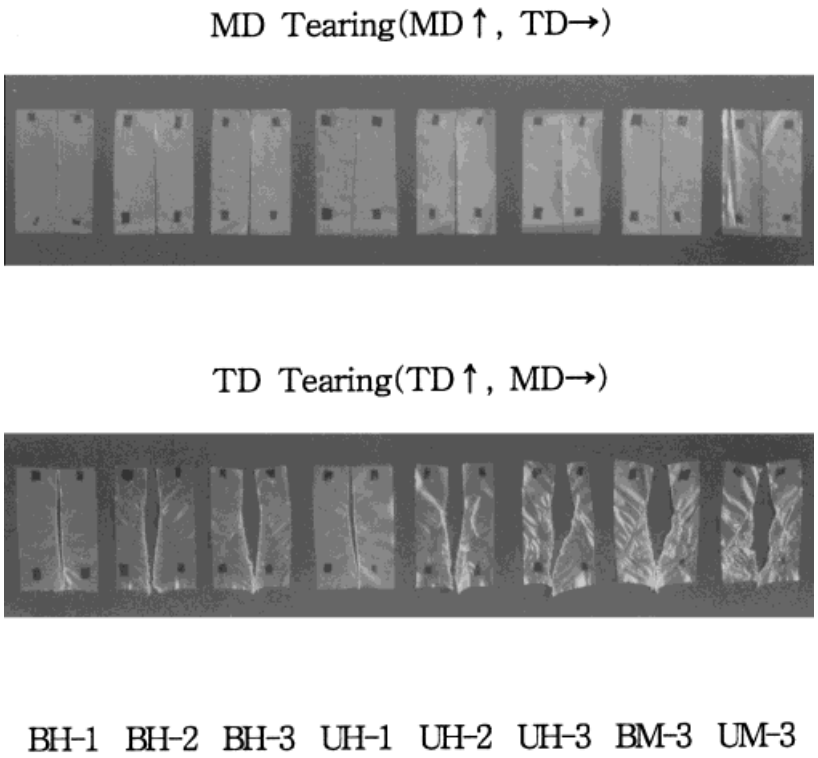

Figure 5 Photographs of the Elmendorf tear failure specimens of the films.

of the resin UH film on the blowing condition is quite similar to that of the resin BH film. However, there are distinctive differences in the structure between the resin BH and the resin UH films prepared under very similar blowing conditions. Compared with the bimodal resin BH film, the corresponding unimodal resin UH film shows less entanglement of the well-developed lamellar stacks (poorly developed network structure) and/or a higher deformation of lamellae in the lamellar stacks (less stable lamellar stacks).

In Figure 4, the scanning electron micrographs of the MMW bimodal resin film BM-3 and the unimodal resin film UM-3 are presented. Figure 4(a) reveals an area of the failure end of the film BM-3. The initial morphology of the films BM-3 and UM-3 is respectively shown on the left side of the micrograph presented in Figure 4(b) and on the right side of the micrograph shown in Figure 4(c). Figure 4(d) is an enlarged micrograph of the deformed region from Figure 4(c). The MMW resin films BM-3 and UM-3 show relatively many cracks between the MD-oriented lamellar stacks, as shown in Figure 4(a)–(c). For the film UM-3, the lamellar stacks reoriented to the TD are highly deformed [Fig. 4(d)]. These results seem to be due to the lower intraconnections and interconnections of the lamellar stacks of the MMW resin films BH-3 and UH-3 than the HMW resin films BH-3 and UH-3.

From the above morphological considerations, we have so far, it may be suggested that the dart drop impact failure of the blown HDPE films is initiated through the separation between lamellar stacks, because the region between the lamellar stacks is weak. This is followed by a rotation of the lamellar stacks, resulting in the axial deformation of the lamellar stacks. Therefore, the dart drop impact resistance of the blown HDPE films seems to be highly associated with the presence of the network structure of the lamellar stacks and the level of intraconnectivity and interconnectivity of the lamellar stacks.

Elmendorf Tear Strength

The Elmendorf tear strength values in the MD and TD of the films are also listed in Table II. For all of the films, the TD Elmendorf tear strength exceeds the MD Elmendorf tear strength. Increasing BUR leads to a better balance of Elmendorf tear strengths in the MD and TD. As shown in Figure 5, the torn edge is well defined and sharp for the MD tearing but sig-

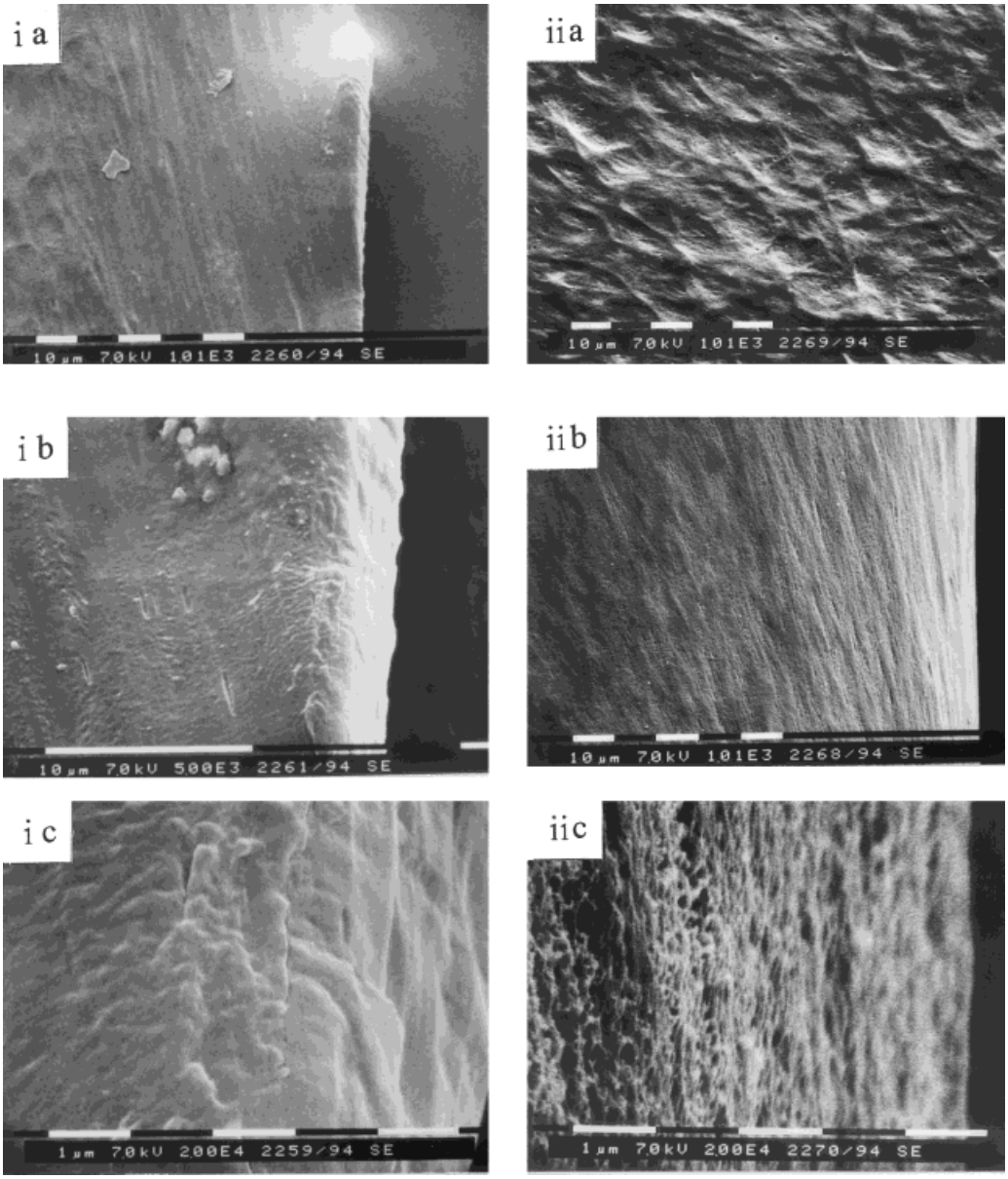

Figure 6 Scanning electron micrographs of the Elmendorf tear failure region of the film BH-1. (i) MD tearing (MD↑, TD→): (a) 1,000×, (b) 5,000×, (c) 20,000×. (ii) TD tearing (TD↑, MD→): (a) an intact area adjacent to the torn edge, 1,000×, (b) 1,000×, (f) 20,000×.

nificantly deformed for the TD tearing. It is also noted that for the TD tearing, the torn edges of the films BH-1 and UH-1 are less deformed than those of the other films. These two films have more random orientation of lamellar stacks than the other films.

In order to understand the above Elmendorf tear behaviors of the films, the morphology of the failure regions was investigated by the use of SEM. As representatives, the scanning electron micrographs of the films BH-1 and BH-2 are presented in Figures 6 and 7, respectively. The films BH-1 and BH-2 correspond to two extreme cases of the orientation distribution of lamellar stacks, as previously mentioned. The sample reference directions, MD and TD, are noted in the figure captions. The higher magnification micrographs (≥5,000×) are enlarged micrographs of the torn edges from the lower magnification micrographs. For example, Figures 6(i b) and 7(ii c) are enlarged micrographs of the torn edges from Figures 6(i a) and 7(ii b), respectively. The orientation

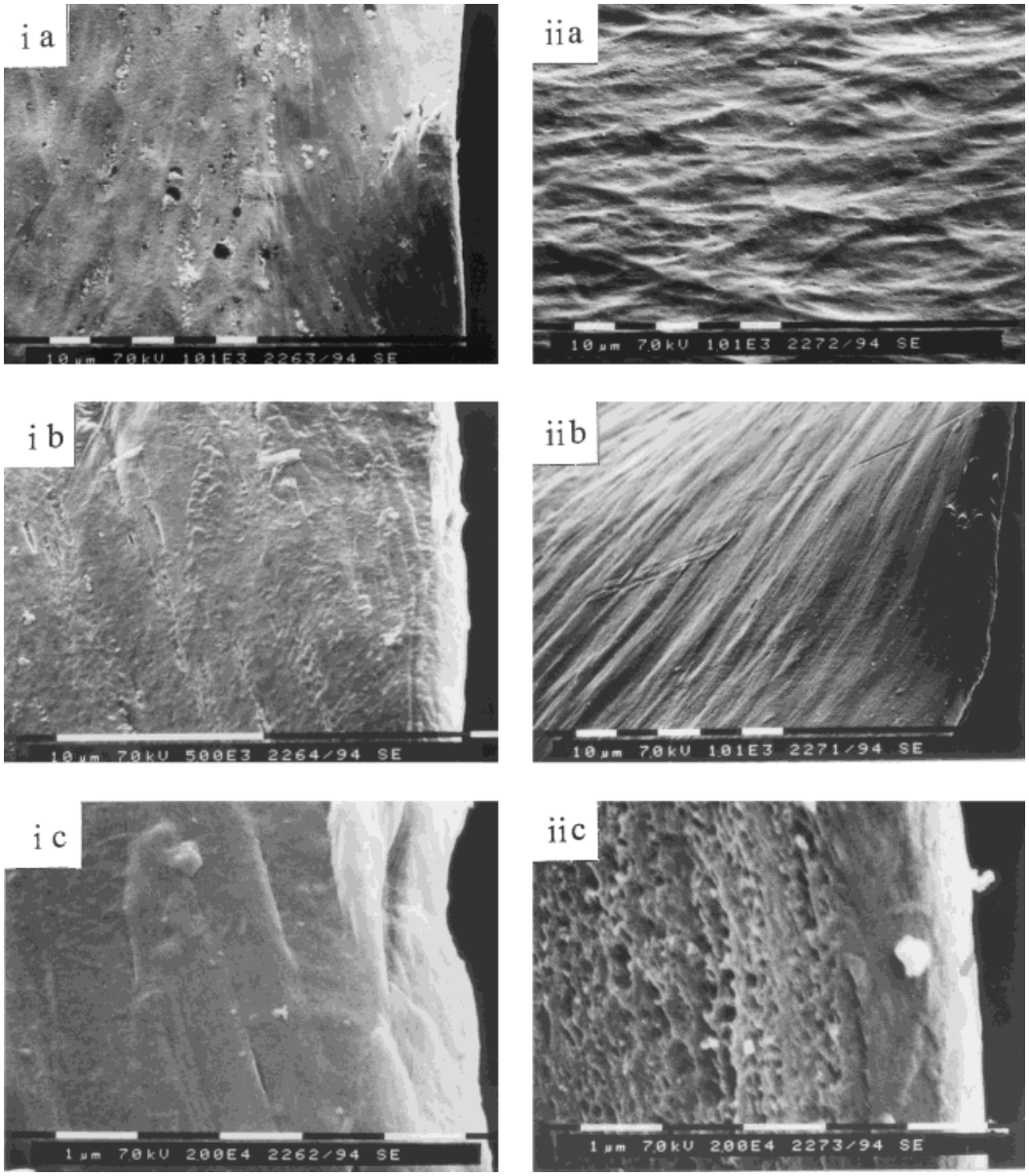

Figure 7 Scanning electron micrographs of the Elmendorf tear failure region of the film BH-2. (i) MD tearing (MD↑, TD→): (a) 1,000×, (b) 5,000×, (c) 20,000×. (ii) TD tearing (TD↑, MD→): (a) an intact area adjacent to the torn edge, 1,000×, (b) 1,000×, (f) 20,000×.

of the lamellar stacks is well revealed at the low-magnification micrographs (1,000×). The higher magnification micrographs (≥5,000×) show the lamellar structure and its deformation. Figure 6(i a) illustrates the size and shape of the MD torn region of the film BH-1. The deformed region is about 70 μm wide (the distance from the torn edge to the end of the intact region). All of the lamellar stacks in the deformed region have preferentially oriented to the tearing direction, MD. The higher magnification micrographs, given in Figure 6(i b) and (i c), reveal that the lamellar stacks have elongated under stress in the MD. Some fracture voids between lamellar stacks are visible in Figure 6(i b). The TD tearing behavior of the film BH-1 is shown in Figure 6(ii). Contrary to the MD tearing, it was very difficult to obtain a scanning electron micrograph which could reveal the torn edge and the initial and deformed morphologies together at a proper magnification, because the deformed zone is highly diffused. The same mechanism of lamellar stacks' rotation parallel to

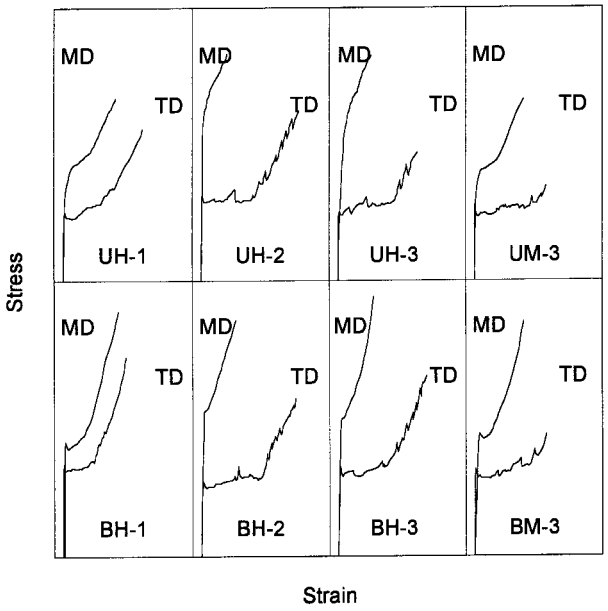

Figure 8 Strain-stress curves of the films. The initial sample thicknesses of the films BH-1, BH-2, BH-3, UH-1, UH-2, UH-3, BM-3, and UM-3 were 25, 22, 26, 22, 26, 25, 26, and 24 μm for the MD and 25, 22, 25, 20, 26, 25, 24, and 24 μm for the TD tensile tests, respectively.

the tearing direction followed by lamellar deformation is observed in Figure 6(ii a) and (ii b), which illustrate respectively the initial and deformed morphologies. The lamellar deformation in the TD tearing is much greater than that in the MD tearing [Fig. 6(ii c) versus (i c)]. The tear behavior of the film BH-2 shows essentially the same feature as that of the film BH-1, except for the lower MD deformation and the higher TD deformation, as shown in Figure 7. On the basis of the above morphological considerations, we can conclude that the tear behavior of the HDPE blown films is highly influenced by the orientation distribution of the lamellar stacks with respect to the tearing direction. The preferential orientation of the lamellar stacks parallel to the MD is responsible for the low tear strength in the MD and the imbalance between the MD and TD tear strengths of the blown HDPE films. This may be due to the higher intercrystalline connectivity along the stack axis direction than along the TD of the lamellar stacks, as demonstrated in the previous study.[11]

Tensile Properties

The stress-strain curves for all of the films are shown in Figure 8. The examination of the plots shows that the stress-strain curves for the films follow one of two basic patterns. One displays an apparent yield point. Beyond this yield point, there is a decrease in the stress with a further increase in elongation. The load then remains approximately constant within a certain range of further elongation. This load then increases continuously until failure occurs as the elongation increases. This pattern will be designated type I. The other, designated type II, shows a poorly defined yield point, and beyond this yield point, there is essentially a continuous increase in stress with elongation. The invariant region for this pattern is either very small or nonexistent. The stress-strain behavior of the films depends highly on the overall processing parameters and the resins used. The deformation process of the blown films seems to be strongly influenced by the orientation of the lamellar stacks, as well as their interconnections, with respect to the tensile direction. Considering the morphology of all of the films, it is clear that the higher coherence of the lamellar stacks to the tensile direction leads to a tendency for the type II deformation. For example, the deformation of the film BH-2 shows the type II in the MD but the type I in the TD. This tensile behavior can be explained by the deformation mechanism proposed by Sherman.[7] He demonstrated a continuous deformation of both the network structure and the lamellar overgrowth of the blown HDPE films. According to the mechanism, lamellar deformation occurred primarily in the region of the lamellar stacks oriented parallel to the tensile direction. The values of yield strength, tensile strength, and elongation at break of the films are also summarized in Table II. On average, tensile strength increases with an increase in the molecular weight of the resins. The anisotropy of the above three key tensile properties of the films seems to be determined by the anisotropy in the orientation distribution of the surface normals of the lamellar stacks at the film plane. The yield and break strengths are higher in the MD than in the TD. The TD elongation is higher than the MD elongation. These results are attributed to the higher preferential orientation of the lamellar stacks to the MD.

CONCLUSIONS

From this comprehensive morphological study of the blown HDPE films, it was found that the dart drop impact failure of the blown HDPE films was

proceeded by initial separations and subsequent reorientations of the lamellar stacks, resulting in the many microfibrils between intrastacks and interstacks. Therefore, the presence of the network structure of the lamellar stacks and the level of intraconnectivity and interconnectivity of the lamellar stacks seem to play a critical role in the dart drop impact resistance of the blown HDPE films. The well-developed network structure of the lamellar stacks should be primarily responsible for a higher dart drop impact resistance of the commercial blown film produced from bimodal HDPE resin. The tearing and tensile deformation behavior of the blown HDPE films seems to be significantly influenced by the orientation distribution of the lamellar stacks, as well as their interconnections, with respect to the tearing and tensile direction. This may be due to the higher intercrystalline connectivity along the stack axis direction than along the TD of the lamellar stacks.

Support of this work by Hanwha Chemical Corporation is gratefully acknowledged.

REFERENCES

1. P. H. Lindenmeyer and S. Lustig, *J. Appl. Polym. Sci.,* **9,** 227 (1965).
2. C. R. Desper, *J. Appl. Polym. Sci.,* **13,** 169 (1969).
3. W. F. Maddams and J. E. Preedy, *J. Appl. Polym. Sci.,* **22,** 2721 (1978).
4. M. A. Macrae and W. F. Maddams, *J. Appl. Polym. Sci.,* **22,** 2761 (1978).
5. D. Hofmann, D. Geiss, A. Janke, G. H. Michler, and P. Fiedler, *J. Appl. Polym. Sci.,* **39,** 1595 (1990).
6. T. Tagawa and K. Ogura, *J. Polym. Sci. Polym. Phys. Ed.,* **18,** 971 (1980).
7. E. S. Sherman, *Polym. Eng. Sci.,* **24,** 895 (1984).
8. E. J. Dormier, J. M. Brady, W. H. Chang, S. D. Schregenberger, and J. D. Barnes, *Proc. ANTEC '89,* 1989, p. 696.
9. D. M. Simpson and I. R. Harrison, *Proc. ANTEC '93,* 1993, p. 1206.
10. K. C. H. Yi and N. J. Maraschin, *Proc. SP'90,* 1990, p. 89.
11. Y. M. Kim, C. H. Kim, J. K. Park, J. W. Kim, and T. I. Min, *J. Appl. Polym. Sci.,* **61,** 1717 (1996).

Received July 27, 1995
Accepted June 1, 1996